Atmosphere-Ocean

ISSN: 0705-5900 (Print) 1480-9214 (Online) Journal homepage: www.tandfonline.com/journals/tato20

# Do Meteorological, Agricultural, and Hydrological Indicators All Point to an Increased Frequency and Intensity of Droughts Across Canada Under a Changing Climate?

Barrie Bonsal, Benita Tam, Xuebin Zhang, Guilong Li, Lisa Philps & Robin Rong

**To cite this article:** Barrie Bonsal, Benita Tam, Xuebin Zhang, Guilong Li, Lisa Philps & Robin Rong (2024) Do Meteorological, Agricultural, and Hydrological Indicators All Point to an Increased Frequency and Intensity of Droughts Across Canada Under a Changing Climate?, Atmosphere-Ocean, 62:5, 372-390, DOI: 10.1080/07055900.2025.2453678

**To link to this article:** https://doi.org/10.1080/07055900.2025.2453678



Published online: 30 Jan 2025.

# Do Meteorological, Agricultural, and Hydrological Indicators All Point to an Increased Frequency and Intensity of Droughts Across Canada Under a Changing Climate?

Barrie Bonsal[1,*], Benita Tam[2], Xuebin Zhang[3], Guilong Li[2], Lisa Philps[2], and Robin Rong[2]

[1]*Watershed Hydrology and Ecology Research Division, Environment and Climate Change Canada, 11 Innovation Boulevard, Saskatoon, Saskatchewan, S7N 3H5, Canada*
[2]*Climate Research Division, Environment and Climate Change Canada, 4905 Dufferin Street, Toronto, Ontario, M3H 5T4, Canada*
[3]*Pacific Climate Impacts Consortium, University House 1, PO Box 1700 Stn CSC, University of Victoria, Victoria, British Columbia, V8W 2Y2, Canada*

[Original manuscript received 16 August 2024; accepted 18 December 2024]

ABSTRACT *Droughts, one of the most significant natural hazards, are complex in nature with varying definitions typically tailored to the timing and/or duration of the episode along with associated impacts. Although previous investigations have assessed future drought occurrence across Canada, none have comprehensively and collectively assessed changes to meteorological, agricultural, and hydrological drought indicators using CMIP6 GCM projections. The main objective of this study was to assess future drought conditions across Canada at various temporal scales using standardized indices representing meteorological, agricultural, and hydrological droughts under multiple shared socio-economic pathways for the near (2041–2060) and far (2081–2100) future. On an annual basis, projected changes to all three drought indicators signify increased drying across the Prairies, portions of interior British Columbia, and most of Ontario. This drying is greater and covers more of the country during the warm season (April to September), while in summer and to a lesser extent autumn, widespread changes are only projected for meteorological and agricultural indicators. In spring, increased dry conditions are only prevalent in meteorological and hydrological indices. The cold season of October to March essentially shows little to no drying in any type of drought. Changes in all drought indices are amplified for higher SSPs and during the late century. This study improves an understanding of the spatial and temporal variations in projected changes to various drought types across Canada in response to human-induced warming. While results from this analysis are applicable for nation-wide drought assessments and drought management plans, they are less suitable for application at local scales where more detailed modelling may be required.*

RÉSUMÉ *[Traduit par la rédaction] Les sécheresses, l'un des risques naturels les plus importants, sont de nature complexe et leurs définitions varient en fonction du moment et/ou de la durée de l'épisode, ainsi que des impacts connexes. Bien que des études antérieures aient évalué l'occurrence future des sécheresses au Canada, aucune n'a évalué de manière exhaustive et collective les changements des indicateurs de sécheresse météorologiques, agricoles et hydrologiques au moyen des projections de l'instrument MIP6 GCM. Le principal objectif de cette étude était d'évaluer les futures conditions de sécheresse au Canada à différentes échelles temporelles en utilisant des indices normalisés représentant les sécheresses météorologiques, agricoles et hydrologiques dans le cadre de multiples scénarios socio-économiques communs pour l'avenir rapproché (2041–2060) et lointain (2081–2100). Sur une base annuelle, les changements prévus pour les trois indicateurs de sécheresse signifient un accroissement de l'assèchement dans les Prairies, dans certaines parties de l'intérieur de la Colombie-Britannique et dans la majeure partie de l'Ontario. Cet assèchement est plus important et couvre une plus grande partie du pays pendant la saison chaude (avril à septembre), tandis qu'en été et, dans une moindre mesure, en automne, des changements généralisés ne sont prévus que pour les indicateurs météorologiques et agricoles. Au printemps, l'augmentation des conditions de sécheresse ne concerne que les indices météorologiques et hydrologiques. La saison froide, d'octobre à mars, présente essentiellement peu ou pas d'assèchement, quel que soit le type de sécheresse. Les changements dans tous les indices de sécheresse sont amplifiés pour les profils socio-économiques*

*Corresponding author's email: barrie.bonsal@ec.gc.ca

*partagés (SSP) les plus élevés et pendant la fin du siècle. Cette étude permet de mieux comprendre les variations spatiales et temporelles des changements prévus pour les différents types de sécheresse au Canada en réponse au réchauffement d'origine humaine. Si les résultats de cette analyse sont applicables aux évaluations des sécheresses à l'échelle nationale et aux plans de gestion des sécheresses, ils sont moins adaptés à une application à l'échelle locale, où une modélisation plus détaillée peut être nécessaire.*

KEYWORDS droughts; Canada; CMIP6; SPEI; soil moisture; runoff

## 1 Introduction

Droughts are arguably one of the most significant natural worldwide hazards. Across Canada, past large-scale, persistent episodes have stressed water availability by depleting soil moisture, reducing stream flows, lowering lake and reservoir levels, and diminishing groundwater supplies. Impacts were felt by most sectors/communities including agriculture, hydro-electricity production, industry, forestry, recreation, aquatic ecosystems, and human health and society. In addition, the environmental impacts from major droughts often include reduced water quality, wetland loss, soil erosion and degradation, increased forest fires, and ecological habitat destruction (e.g. Bonsal et al., 2011).

Droughts are a part of natural climatic variability. They begin as meteorological types, which involve a lack of precipitation that can be exacerbated by anomalously high temperatures. Meteorological droughts are frequently assessed using atmospheric-based drought indices that combine precipitation and some measurement of evaporative demand (normally by estimating potential evapotranspiration (PET)), the latter being imperative to understand the growing threat of human-induced warming. PET is subtracted from precipitation to calculate a drought index such as the Standardized Precipitation Evapotranspiration Index (SPEI) (Vicente-Serrano, Beguería, & López-Moreno, 2010; Beguería et al., 2014).

Depending on the timing and duration, meteorological droughts can propagate through to agricultural/ecological types because of inadequate soil moisture leading to decreased crop yields and terrestrial ecosystem stress such as forest mortality. These droughts are best represented by soil moisture since deficiencies can directly lead to plant water stress (Beguería et al., 2014; Chen et al., 2020; Hayat et al., 2019). However, there are few direct soil moisture measurements available and, therefore, amounts are often estimated through remote sensing and/or modelling. Future changes in soil moisture are primarily assessed using direct soil moisture output from climate models that include surface (∼top 10 cm) and total soil moisture, the former being more susceptible to widespread drying than total, which includes carry-over of moisture from previous seasons deeper in the soil column (Berg et al., 2017; Kumar et al., 2019).

Hydrological droughts refer to a lack of water that is usually represented by low levels in streams, lakes, reservoirs, and groundwater (Van Loon, 2015). Drivers of surface water deficits, however, are complex and highly dependent on watershed characteristics (e.g. size, relief, soil properties, vegetation, storage, presence of dams, and diversions) (e.g. Jehanzaib et al., 2020; Tijdeman et al., 2018; Van Loon et al., 2016). Cryospheric conditions, including snow, glaciers, and permafrost, also strongly impact the amount and timing of surface runoff, particularly in Canada (e.g. Bonsal et al., 2019; Derksen et al., 2019). Approaches to assessing projected changes in hydrological deficits under anthropogenic warming are varied. Some studies examined future stream flow projections through the incorporation of hydrological models forced by climate model output (Budhathoki et al., 2022; Islam et al., 2019; Schnorbus, 2020; Shrestha et al., 2019; Stadnyk et al., 2021). Another approach involves using simulated runoff directly from the land surface component of climate models, which are tightly coupled to simulate climatic and hydrological processes (e.g. Arora & Boer, 2001; Seiler et al., 2021; Sigmond et al., 2023; Zhang et al., 2014). While the latter approach has some limitations (e.g. coarser resolution, model biases), it does provide robust information on simulated changes that may be useful for nation-wide assessments and adaptation measures (Arora et al., 2025).

Meteorological, agricultural, and hydrological droughts are driven by moisture deficits in different aspects of the water cycle, and thus, do not necessarily provide the same results or insight on the effects of climate change. For example, Zeng et al. (2022) assessed future CMIP6 projected global meteorological, hydrological, and agricultural drought using Standardized Precipitation Index (SPI) and SPEI (meteorological), Standardized Runoff Index (SRI) (hydrological), and Standardized Soil Moisture Index (SSI) (agricultural). They found that the different types of droughts generally exhibited longer durations, larger spatial extent, and greater severity farther into the future with SPEI showing the largest increase. In another global study, Vicente-Serrano et al. (2020) also used several drought indices to assess future changes to meteorological, hydrological, and agricultural drought. They determined that climatological and hydrological droughts are likely to undergo similar temporal evolution during the twenty-first century, with almost 30% of the global land areas experiencing water deficit under future greenhouse gas emissions scenarios.

Across Canada, most historical and projected future drought studies have focused on meteorological drought indicators (e.g. SPI, SPEI) and inferred agricultural and hydrological drought from these indices. For future drought, many regional and Canada-wide studies revealed an overall consistency towards the increased likelihood of drought events over southern interior continental regions of Canada, especially during summer, under higher warming emission scenarios (Bonsal et al., 2013; Dibike et al., 2017; Masud et al., 2017; Tam et al., 2019; Tam, Bonsal et al., 2023). A regional investigation by Zare et al. (2023) evaluated future meteorological and

agricultural drought in the South Saskatchewan River Basin of the Canadian Prairies and found that meteorological drought duration and severity will exceed historical values. Agricultural drought indices showed more significant droughts compared with meteorological drought indices (Zare et al., 2023).

Although previous investigations have assessed future drought occurrence across Canada under a changing climate, none have specifically and comparatively focused on future changes to meteorological, agricultural, and hydrological droughts across the entire country. For example, Tam, Bonsal et al. (2023) assessed CMIP6 meteorological drought projections across Canada, but not with hydrological or agricultural drought indicators. Thus, using output from 22 of the latest CMIP6 global climate models (GCMs), the main objective of this study was to provide a comprehensive assessment of future drought changes across Canada at various temporal scales. This involved the incorporation of standardized indices representing meteorological (SPEI), agricultural (SSI), and hydrological (SRI) droughts using multiple shared socio-economic pathways (SSPs) for the near future (2041–2060) and far future (2081–2100) periods.

## 2 Data and methods

### a *Data*

Three indices representing meteorological, agricultural, and hydrological drought were calculated using output from 22 Coupled Model Intercomparison Project Sixth Phase (CMIP6) (Eyring et al., 2016) GCMs for three SSPs: SSP1-2.6, SSP2-4.5, and SSP5-8.5 (Meinshausen et al., 2020) (Table 1). The GCMs were chosen based on data availability and were similar to those incorporated by Tam, Bonsal et al. (2023) in their assessment of various PET methods to calculate meteorological droughts across Canada using SPEI. Note that the hydrological drought (runoff) ensemble projections excluded the ACCESS-CM2, ACCESS-ESM1-5, CanESM5, GFDL-ESM4, and MRI-ESM2-0 GCMs due to poor distribution fit that resulted in grid cell values of zero.

TABLE 1. Global Climate Models and realizations used to calculate SPEI, SSI, and SRI drought indicator ensembles. Note that for SRI, ACCESS-CM2, ACCESS-ESM1-5, CanESM5, GFDL-ESM4, and MRI-ESM2-0 were excluded from the ensembles due to poor distribution fit.

| | Model (realization) | References |
|---|---|---|
| 1. | ACCESS-CM2 (r1i1p1f1) | Bi et al. (2020) |
| 2. | ACCESS-ESM1-5 (r1i1p1f1) | Ziehn et al. (2020) |
| 3. | CanESM5 (r1i1p2f1) | Swart et al. (2019) |
| 4. | CMCC-ESM2 (r1i1p1f1) | Cherchi et al. (2019); Lovato et al. (2022) |
| 5. | CNRM-CM6-1 (r1i1p1f2) | Voldoire et al. (2019); Saint-Martin et al. (2021) |
| 6. | CNRM-ESM2-1 (r1i1p1f2) | Séférian et al. (2019) |
| 7. | EC-Earth3 (r4i1p1f1) | Döscher et al. (2022) |
| 8. | EC-Earth3-Veg (r1i1p1f1) | |
| 9. | GFDL-ESM4 (r1i1p1f1) | Dunne et al. (2020) |
| 10. | HadGEM3-GC31-LL (r1i1p1f3) | Kuhlbrodt et al. (2018); Williams et al. (2018) |
| 11. | INM-CM4-8 (r1i1p1f1) | Volodin et al. (2018) |
| 12. | INM-CM5-0 (r1i1p1f1) | Volodin et al. (2017) |
| 13. | IPSL-CM6A-LR (r1i1p1f1) | Boucher et al. (2020) |
| 14. | MIROC6 (r1i1p1f1) | Tatebe et al. (2019) |
| 15. | MIROC-ES2L (r1i1p1f2) | Hajima et al. (2020) |
| 16. | MPI-ESM1-2-HR (r1i1p1f1) | Müller et al. (2018) |
| 17. | MPI-ESM1-2-LR (r1i1p1f1) | Mauritsen et al. (2019) |
| 18. | MRI-ESM2-0 (r1i1p1f1) | Mizuta et al. (2012); Yukimoto et al. (2019) |
| 19. | NorESM2-LM (r1i1p1f1) | Seland et al. (2020) |
| 20. | NorESM2-MM (r1i1p1f1) | |
| 21. | TaiESM1 (r1i1p1f1) | Lee et al. (2020) |
| 22. | UKESM1-0-LL (r1i1p1f2) | Sellar et al. (2019) |

Based on Tam, Bonsal et al. (2023), the current study used SPEI as a measure of meteorological drought with PET calculated with the Penman-Monteith method (which incorporates wind speed, humidity, radiation, and air temperature from the various GCMs). Temperature and precipitation were bias corrected prior to the calculation of SPEI (see Tam, Bonsal et al. (2023) for details). Agricultural drought was represented by GCM-derived total soil moisture content with the different phases summed over all layers in kg $m^{-2}$. Hydrological drought was determined using GCM-derived surface runoff leaving the land portion of the grid cell, excluding drainage through the base of the soil model (in mm $day^{-1}$). The period of GCM simulations was from 1950 to 2100. All output variables were regridded to a common 1 degree by 1 degree resolution prior to the calculation of the various drought indices. Each index was standardized using the baseline reference period, 1950–2014. For agricultural and hydrological droughts, standardized surface (10 cm) soil moisture and standardized total runoff results were also produced and are available upon request.

### b *Standardization and Distribution Testing*

SPEI was calculated using the same procedure as Tam, Bonsal et al. (2023). One of the advantages of SPEI is that it is simplistic yet multi-scalar. A standardized index such as SPEI allows for spatiotemporal comparisons across diverse regions. Therefore, total soil moisture (SSI) and surface runoff (SRI) were also standardized to a normal distribution. This also allows for easier comparison among the different drought indicators. To select the appropriate probability distribution required to transform total soil moisture and surface runoff projections, the fit of multiple historical simulations per model was assessed using generalized logistic (GLO), generalized extreme value (GEV), Pearson Type 3 (PE3), and normal (NOR) distributions.

The GCMs used in the distribution analysis are in Table 1. Up to three historical runs per GCM were examined (depending on availability) across four time scales: 1, 3, 12, and 24 months. The four candidate probability distributions (GLO, GEV, PE3, and NOR) were assessed by looking at the goodness of fit of each historical simulation (over 1950–2014) per model for total soil moisture and surface runoff using the Kolmogorov–Smirnov (KS) test. The distribution with the lowest overall rejection rates across the models for both variables was chosen as the

probability distribution function. From the KS test results, GEV was selected as the probability distribution for surface runoff, and PE3 for total soil moisture. Each variable was standardized to a normal distribution with a mean = 0 and standard deviation = 1 using a baseline reference period of 1950–2014. Standardized results therefore represent the number of standard deviations from which the transformed variable departs from mean values over the reference period. Standardized indices should be interpreted as a relative measure of water surplus (positive values) or deficit (negative values) with respect to hydroclimate conditions of the chosen reference period (1950–2014). A negative value indicates dryness and a positive value indicates wetness. A reference period of 1950–2014 was used because a minimum of 30 years is generally recommended for parameter estimation, and at least 60 years for stable estimates at distribution tails (Guttman, 1994, 1999; McKee et al., 1993).

**c** *Drought Indicator Analyses*

Several temporal periods were considered in the analyses of the different drought types. Annual events were assessed during the 12-month agricultural year (September to August) while 6-month droughts were examined during the warm season (April to September) and cold season (October to March). Seasonal periods were also assessed including spring (March to May), summer (June to August), and autumn (September to November). For these temporal periods, changes in each of the standardized indices (SPEI, SSI, SRI; relative to the 1950–2014 period) were presented for each SSP during the near (2041–2060) and far (2081–2100) future. These changes provided a relative measure of how general drought conditions are projected to change (i.e. which regions become drier and by how much) for each drought type.

Further insight into drought changes was provided by examining how often the current 1 in 10-year drought event (based on the 1950–2014 period) occurs in the future. This is carried out by assessing the probability of exceedance over a 10-year period using SPEI, SSI, and SRI projections. The threshold of exceedance was calculated based on an exceedance probability of 10% of a normal distribution (−1.28). Once the frequency of threshold exceedances was calculated, the probability of exceedance in a 10-year period was produced using the following formula:

$$P = n/N*10$$

where $P$ is the probability of exceedance, $n$ is the number of times the drought index exceeds the threshold, and $N$ is the total number of years. This measure provided an indication into future changes of less frequently occurring (i.e. moderate to major) droughts.

To provide proper context regarding future drought changes relative to current climate, modelled baseline (1950–2014), non-standardized conditions for each drought indicator were examined. Meteorological baseline conditions were represented by precipitation minus PET ($P$ minus PET in mm), agricultural drought by average total soil moisture (in kg $m^{-2}$), and hydrological drought by average surface runoff (in mm $day^{-1}$).

## 3 Results

**a** *Baseline Conditions*

Modelled historical baseline conditions of meteorological ($P$ minus PET), agricultural (average total soil moisture), and hydrological (average surface runoff) drought are shown in Fig. 1, which includes the average ensemble median (for all GCMs) of baseline conditions on (a) annual, (b) warm season, (c) cold season, and (d–f) seasonal periods.

Annually, baseline $P$ minus PET shows moisture deficits (i.e. negative $P$ minus PET) across all three Prairie provinces, interior British Columbia, and much of the Northwest Territories (excluding the high Arctic Islands) (Fig. 1a). Greatest deficits occur in the extreme southern Prairies. The rest of the country is associated with a moisture surplus with the highest values on the far west coast. Baseline total soil moisture has a more varied pattern including higher average values in central British Columbia, western Northwest Territories, northern Alberta, and along the southern coast of Hudson Bay. Lowest values are in southern regions of Alberta, Saskatchewan, and Ontario. For baseline surface runoff, highest values are located on the Pacific and Atlantic coasts with lowest amounts through west-central Canada and the high Arctic Islands. The preceding reveals that on an annual basis, these three indicators vary across the country. The southern Prairies tend to have the lowest values in all three indicators particularly for $P$ minus PET. Extreme western and Atlantic regions of Canada, along with the high Arctic Islands are primarily the wettest areas with the rest of Canada showing more varied results depending on the indicator.

Geographical patterns for the 6-month warm season (Fig. 1b) are similar to the annual except that a larger area of Canada (in fact most of the country) is associated with a moisture deficit as represented by $P$ minus PET. Total soil moisture is again highest in central British Columbia, western Northwest Territories, northern Alberta, and along the southern coast of Hudson Bay, while surface runoff is greatest along the west and east coasts.

Fig. 1c reveals that the 6-month cold season conditions are considerably different regarding meteorological and, to a lesser extent, hydrological conditions. However, a similar pattern to that of the warm season exists with respect to total soil moisture. The meteorological pattern generally shows moisture surplus across Canada except for deficits in a small region of southern Alberta and Saskatchewan and higher surpluses along the mountainous regions of the west coast and the British Columbia–Alberta border. Surface runoff is quite low for almost the whole country except for the west coast of British Columbia and parts of the Maritimes.

On a seasonal basis, all three indicators during spring (Fig. 1d) closely resemble the annual and warm season pattern.

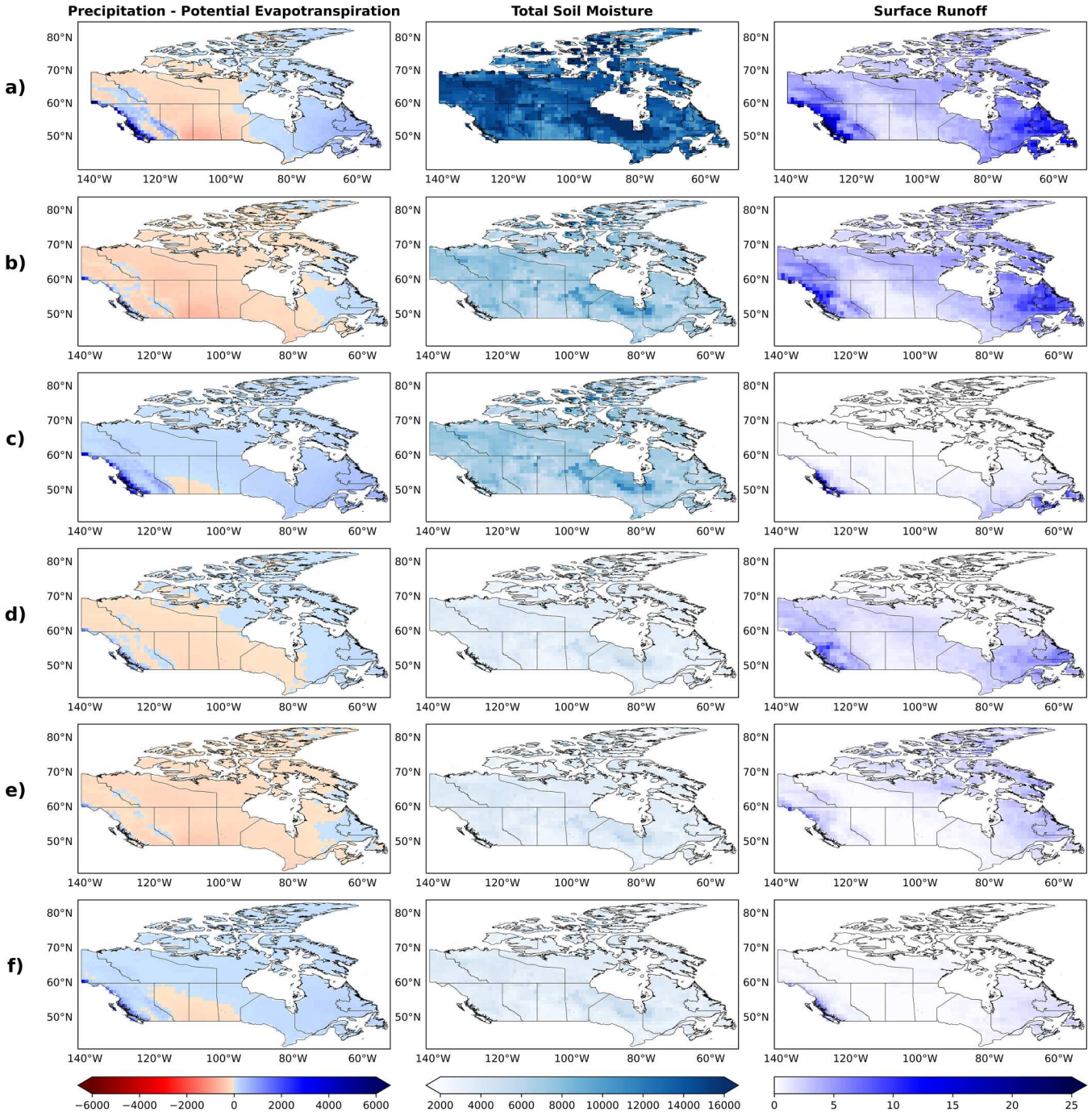


Fig. 1 Average ensemble median (for all GCMs) projections of meteorological (*P* minus PET in mm), agricultural (average total soil moisture in kg $m^{-2}$), and hydrological (average surface runoff in mm $day^{-1}$) baseline conditions (1950–2014) on (a) annual (September to August), (b) warm season (April to September), (c) cold season (October to March), and seasonal (d) spring: March–April–May, (e) summer: June–July–August, (f) autumn: September–October–November periods.

Summer (Fig. 1e) is somewhat drier for all drought types as compared to spring, however, the spatial pattern is consistent with spring conditions. Autumn (Fig. 1f) is quite different from the other seasons with respect to meteorological conditions, with its pattern more closely resembling those of the cold season in Fig. 1c. The other two indicators reveal small values with similar patterns to the spring and summer.

### b *Future Annual Changes*

#### 1 SPEI, SSI, AND SRI

Fig. 2 provides projected annual SPEI, SSI, and SRI changes across Canada for three SSPs during (a) mid-century (2041–2060), and (b) late century (2081–2100) periods. For SPEI, lower values (i.e. drier conditions) mainly occur across central Canada (Alberta through most of Ontario and the

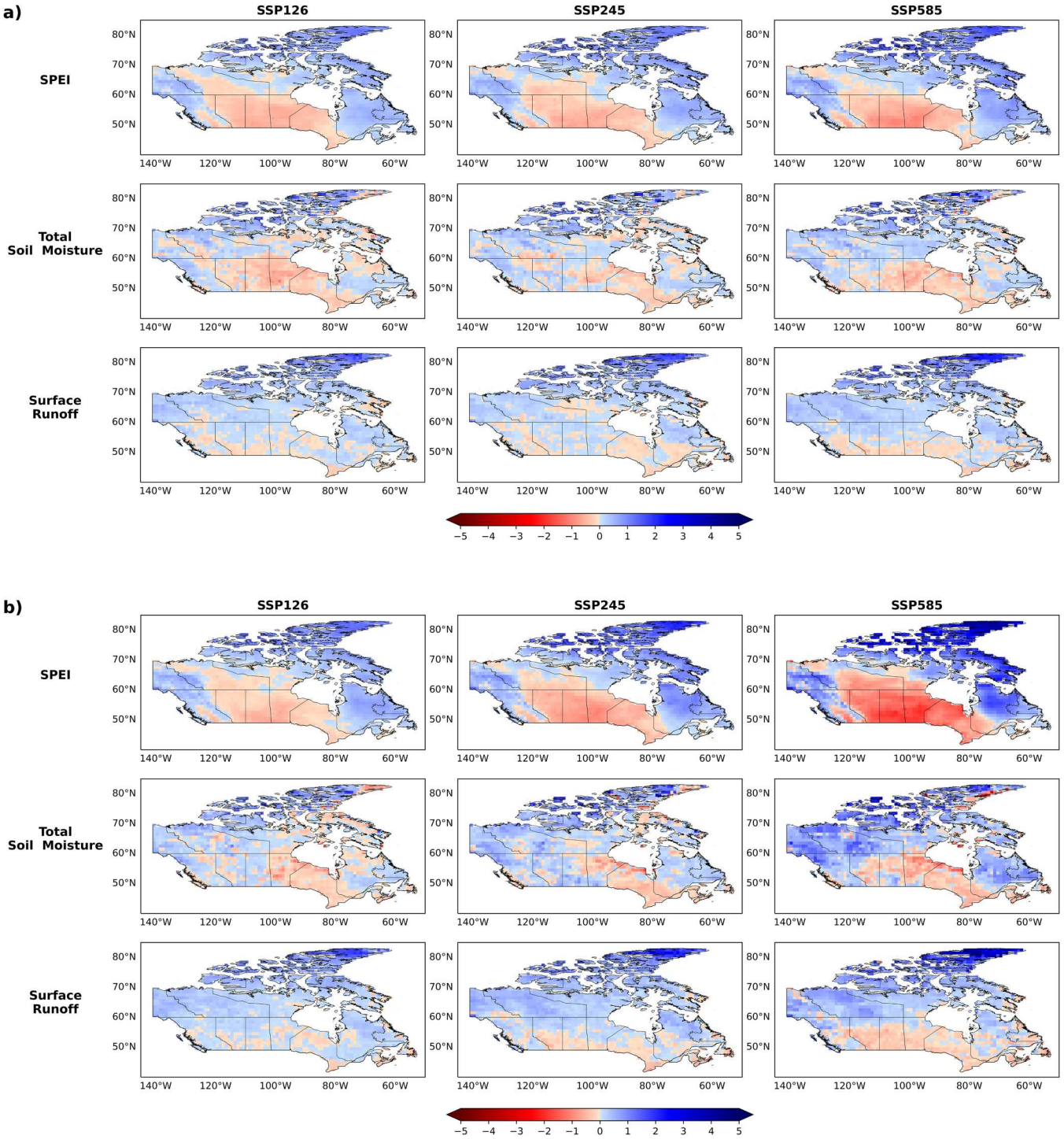


Fig. 2 Average ensemble median (for all GCMs) projections of annual (September to August) SPEI, SSI, and SRI using SSPs 1-2.6, 2-4.5, and 5-8.5 for (a) 2041–2060 and (b) 2081–2100.

southern Northwest Territories), along with interior British Columbia. The changes are greater in more southern areas of this region and are amplified for higher SSPs and during the late century. Across most of the Prairies and interior British Columbia, the average standardized SPEI value for SSP5-8.5 at the end of the century is around −2.0. With the exception of Ontario, the regions with projected decreases in SPEI occur in areas that currently have a $P$ minus PET deficit (Fig. 1a). Therefore, these already meteorologically dry regions are projected to become even drier in the future.

The changes in SSI are geographically similar to those associated with SPEI. In terms of total soil moisture, the

greatest changes involve reduced amounts concentrated mainly in Manitoba, Ontario and parts of the Prairies. These areas of reduced soil moisture also showed decreases in SPEI, thus signifying an increase in both meteorological and agricultural droughts on an annual scale. As with SPEI, the agricultural changes are amplified for higher SSPs but are consistent for the near and far future time periods.

SRI shows the least drying among all the indicators. Slightly drier conditions are scattered throughout the approximate southern third of the country, while the rest of Canada is associated with wetter conditions that amplify in a northern direction. The drier areas associated with SSP5-8.5 at the end of the century mostly overlap areas that are projected to have decreases in SPEI and SSI, thus indicating that all three types of droughts will increase in the southern Prairies and most of Ontario for higher emissions.

#### 2 1 IN 10-YEAR EVENTS

Projected ensemble changes to 1 in 10-year annual drought events for each indicator and SSP are provided in Fig. 3 for (a) 2041–2060 and (b) 2081–2100. Overall, the spatial pattern is similar to the average changes shown in Fig. 2. For SPEI, the extreme southern Prairies are associated with the most drastic changes. For example, under the SSP5-8.5 emission scenario for 2081–2100, the current 1 in 10-year drought increases to approximately 6 or 7 times every 10 years. Even the lowest emission scenario (SSP1.2-6) shows an increase of around 2–3 occurrences every 10 years, thus signifying a substantial increase in the frequency of future drought. Mid-century changes are spatially similar but less pronounced.

The agricultural drought indicator also shows substantial future changes to 1 in 10-year events, particularly through the Canadian Prairies, extreme northern Ontario and the Northwest Territories (increases to ∼4 to 7 occurrences per 10 years at the end of the century for SSP5.8-5).

As with average change (Fig. 2), SRI shows the least amount of change with respect to 1 in 10-year occurrences. For the most part, all 3 indicators show increases in 1 in 10-year drought events over most of the country, even for SSP1-2.6 in the near future (∼1 to 2 events). These increases amplify for higher emission scenarios and towards the end of this century.

### c *Future 6-Month Changes*

#### 1 WARM SEASON SPEI, SSI, AND SRI

During the April through September period, SPEI changes are generally more widespread compared to annual with drier conditions covering most of Canada except for the extreme northwest and Arctic Islands (Fig. 4). These changes are particularly amplified at the end of the century under SSP5.8-5, especially in central Canada (SPEI <−1.5).

For soil moisture, the spatial and temporal patterns are also more widespread compared to the annual maps with pronounced drying across a majority of the country (∼south of 60°). The changes are amplified for higher SSPs and during the late century.

Runoff is considerably lower when compared to annual with drier conditions projected across most of Canada with the exception of the high Arctic Islands. Driest regions include British Columbia, central Ontario and Quebec, and the Maritimes. For all three indicators, warm season drought indicators of all types suggest projected drought increases over most regions of Canada, which is consistent with several studies that have indicated an increased risk to future freshwater supplies during the warm season across the country (e.g. Bonsal et al., 2019).

#### 2 WARM SEASON 1 IN 10-YEAR EVENTS

Fig. 5 displays projected changes to the 1 in 10-year occurrence of warm season droughts across Canada. The patterns are similar to annual SPEI, SSI, and SRI 1 in 10-year changes. However, during the warm season, there are considerably more occurrences for all types of droughts, especially for high emissions at the end of the century. This is particularly evident for surface runoff where a substantial increase in the 1 in 10-year event is projected, especially in British Columbia.

#### 3 COLD SEASON SPEI, SSI, AND SRI

For the most part, Fig. 6 shows that during the cold season of October to March, there are very few projected decreases in three drought indicators. Slight decreases are projected for total soil moisture mostly across the Prairies, northwestern Ontario and parts of the Northwest Territories and Nunavut for all emission scenarios and time periods. For SPEI, the only region of drying is in the extreme southern Prairies. Everywhere else is projected to have meteorological moisture surpluses. In terms of SRI, almost none of Canada shows drier conditions (except for extreme southern Ontario and parts of Nova Scotia, and to a lesser degree southern Alberta). All other regions are projected to have considerably more cold-season runoff.

#### 4 COLD SEASON 1 IN 10-YEAR EVENTS

The spatial patterns of changes to 1 in 10-year drought occurrences during the cold season (Fig. 7) are similar to those in Fig. 6. Greatest differences are again associated with total soil moisture, particularly in the Prairies and the Northwest Territories. Increases in meteorological droughts are only projected for the southern Prairies, while cold season runoff shows no discernible pattern. As with all other projections, impacts are greater for higher emission scenarios and at the end of the century.

### d *Future Seasonal Changes*

#### 1 SPRING SPEI, SSI, AND SRI AND 1 IN 10-YEAR EVENTS

Fig. 8 shows projected average spring SPEI, SSI, and SRI, and 1 in 10-year drought occurrence changes for the three SSPs during the late century. To a large extent, the patterns in both Fig. 8a and b resemble those of the annual results (Figs 2 and 3). SPEI and SRI spring patterns also resemble

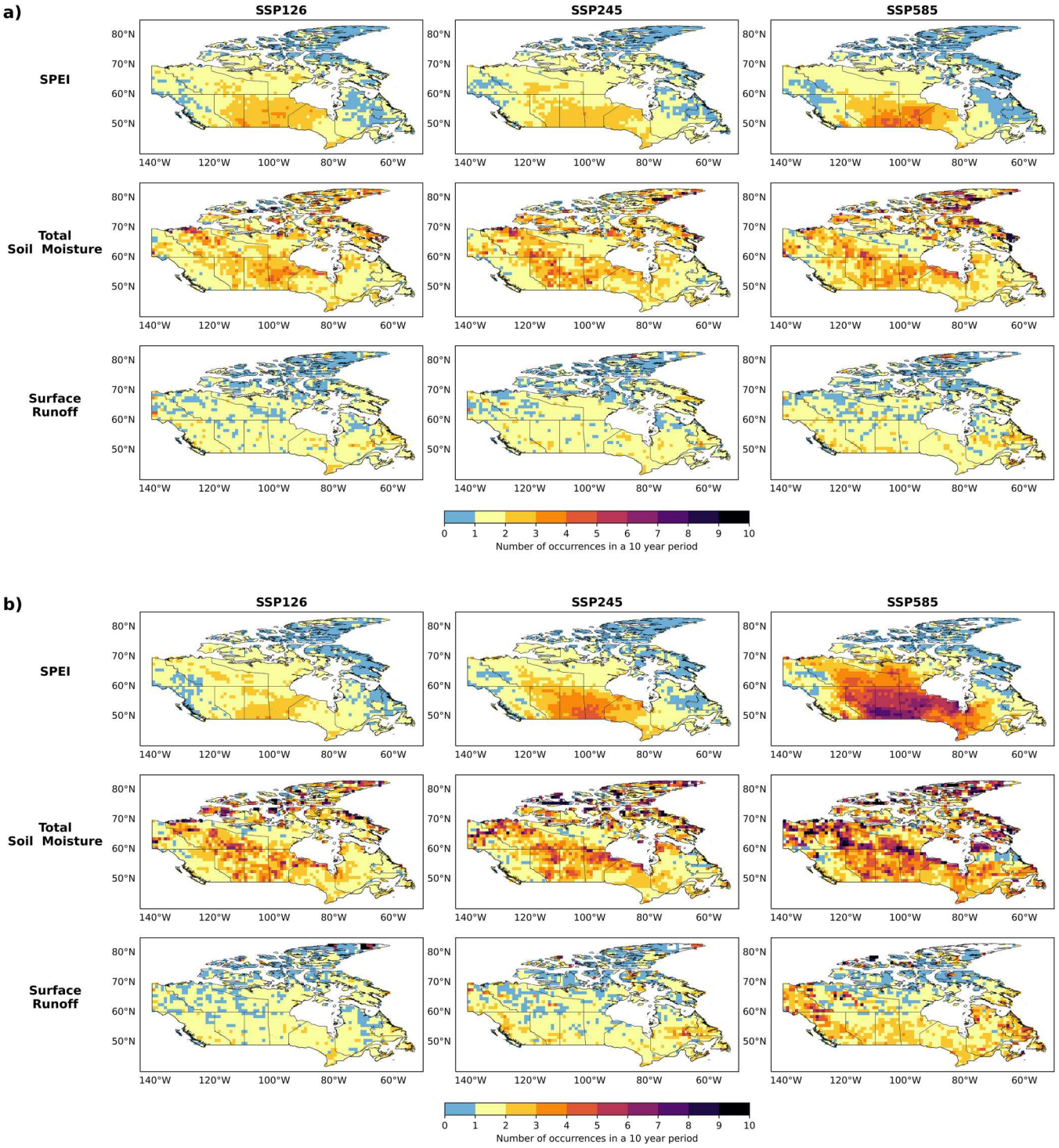


Fig. 3 Average ensemble median (for all GCMs) projections of changes to baseline (1950–2014) 1 in 10-year annual drought occurrences for SPEI, SSI, and SRI using SSPs 1-2.6, 2-4.5, and 5-8.5 for (a) 2041–2060 and (b) 2081–2100.

the warm season (Fig. 4) but are less pronounced. Total soil moisture shows the least drying when compared to the other two indicators (particularly in average conditions) (Fig. 8a). Unlike other periods, surface runoff projections show the greatest drying of all the indicators.

## 2 SUMMER SPEI, SSI, AND SRI AND 1 IN 10-YEAR EVENTS

For meteorological and agricultural indicators, Fig. 9 reveals that the patterns and intensities are almost identical to the warm season (Figs 4 and 5). Hydrological changes are inconsistent and less pronounced, even showing wetting in some

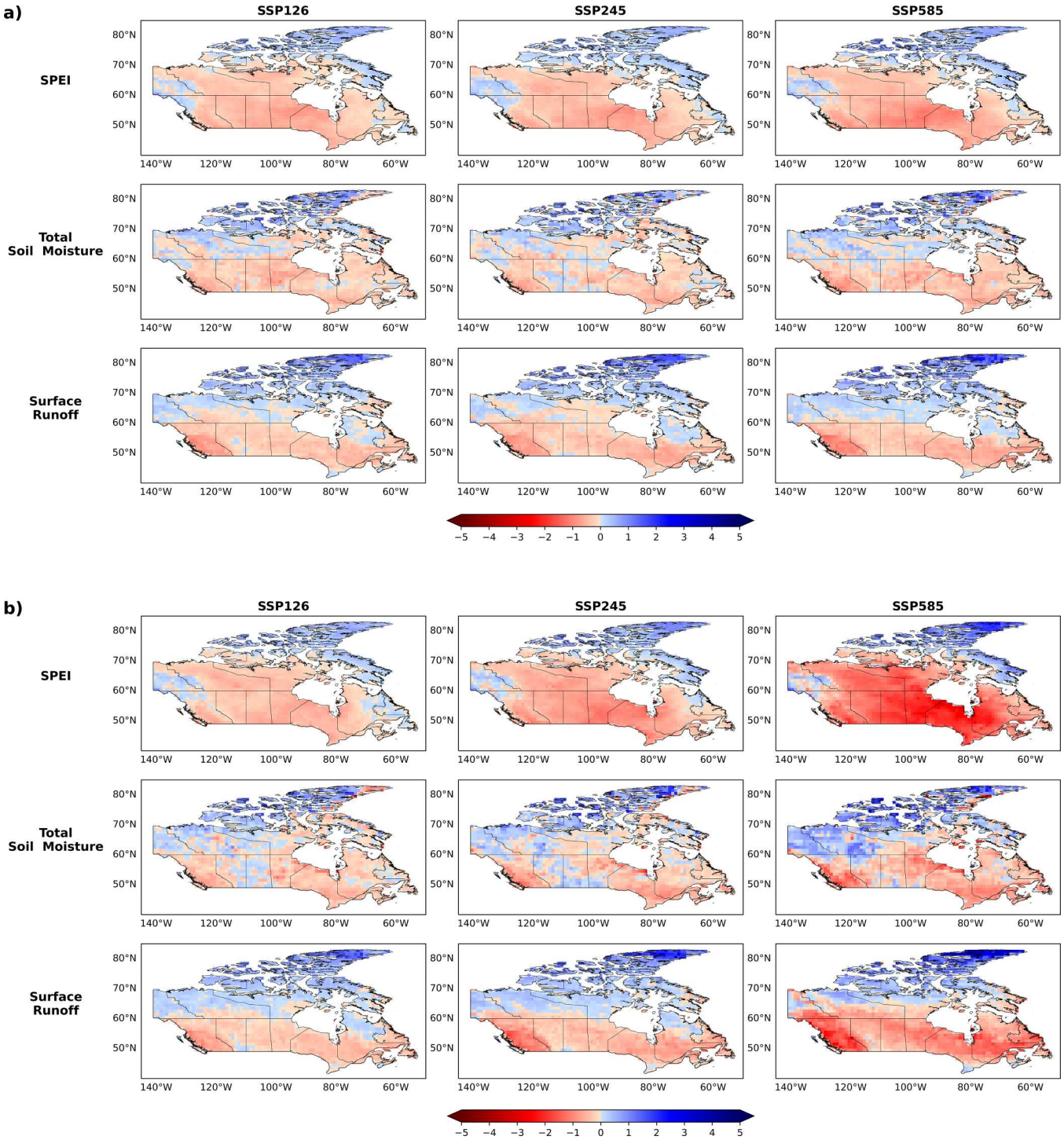


Fig. 4 Same as Fig. 2 except for warm season (April to September).

regions. For changes in 1 in 10-year occurrences, there are very large projected changes to SPEI and total soil moisture approaching 7–8 occurrences per decade in some regions under the highest emission scenario. Surface runoff once again shows less change.

## 3 AUTUMN SPEI, SSI, AND SRI AND 1 IN 10-YEAR EVENTS

The Sep-Oct-Nov period (Fig. 10) shows a closer likeness to the cold season; however, the drying is more pronounced and widespread during autumn for SPEI and total soil moisture for both average and 1 in 10-year drought occurrences. Runoff shows

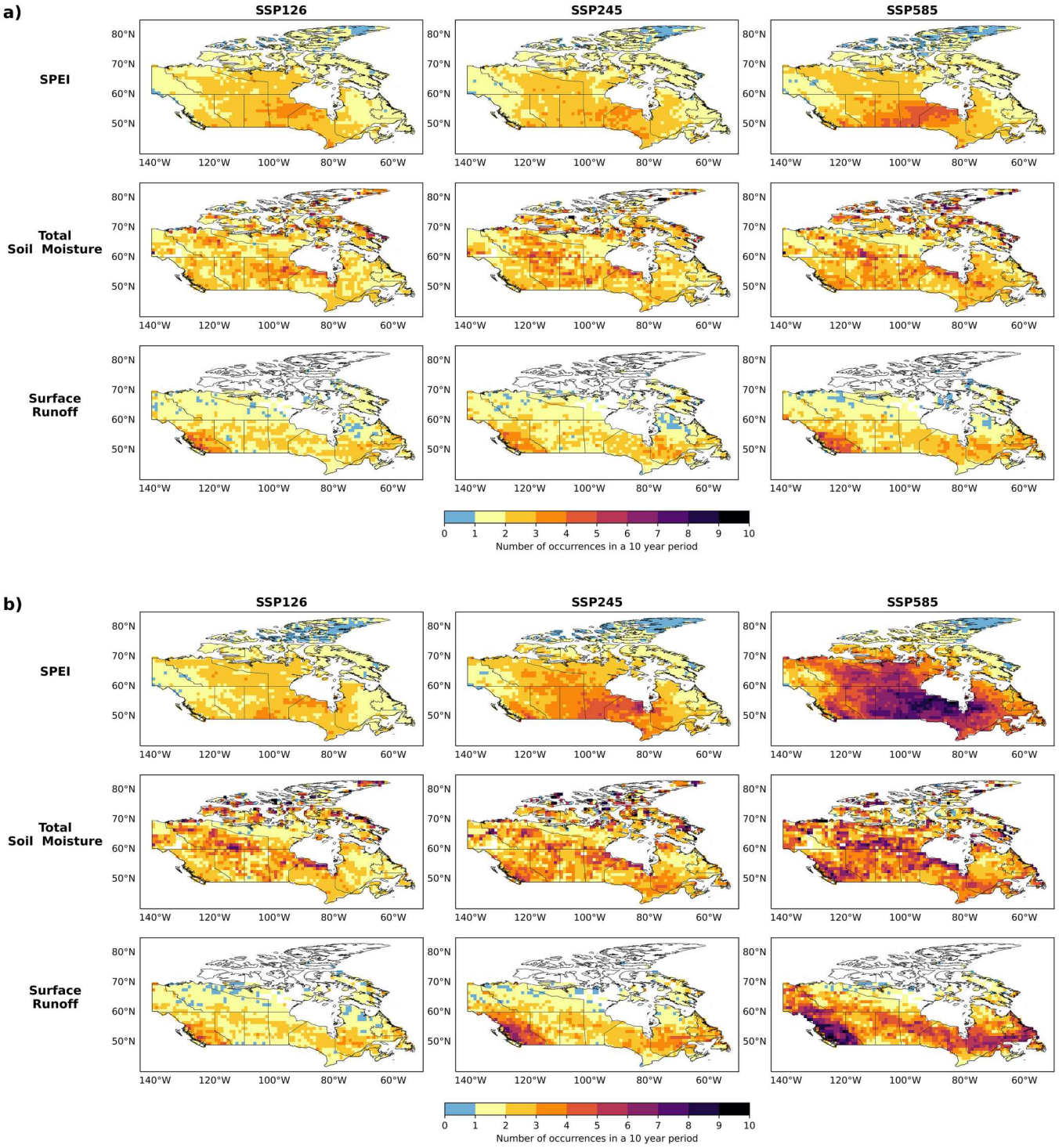


Fig. 5 Same as Fig. 3 except for warm season (April to September).

no autumn drying for average changes and an inconsistent pattern with relatively no change for 1 in 10-year occurrences.

## 4 Discussion

The preceding assessed changes to the intensity and frequency of different drought indicators using output from numerous CMIP6 GCMs with multiple SSPs. On an annual basis, projected changes to SPEI suggest increases in the intensity and frequency of meteorological droughts mainly across central Canada (Alberta through most of Ontario and the southern Northwest Territories), along with interior British Columbia (Figs 2 and 3). This is consistent with similar

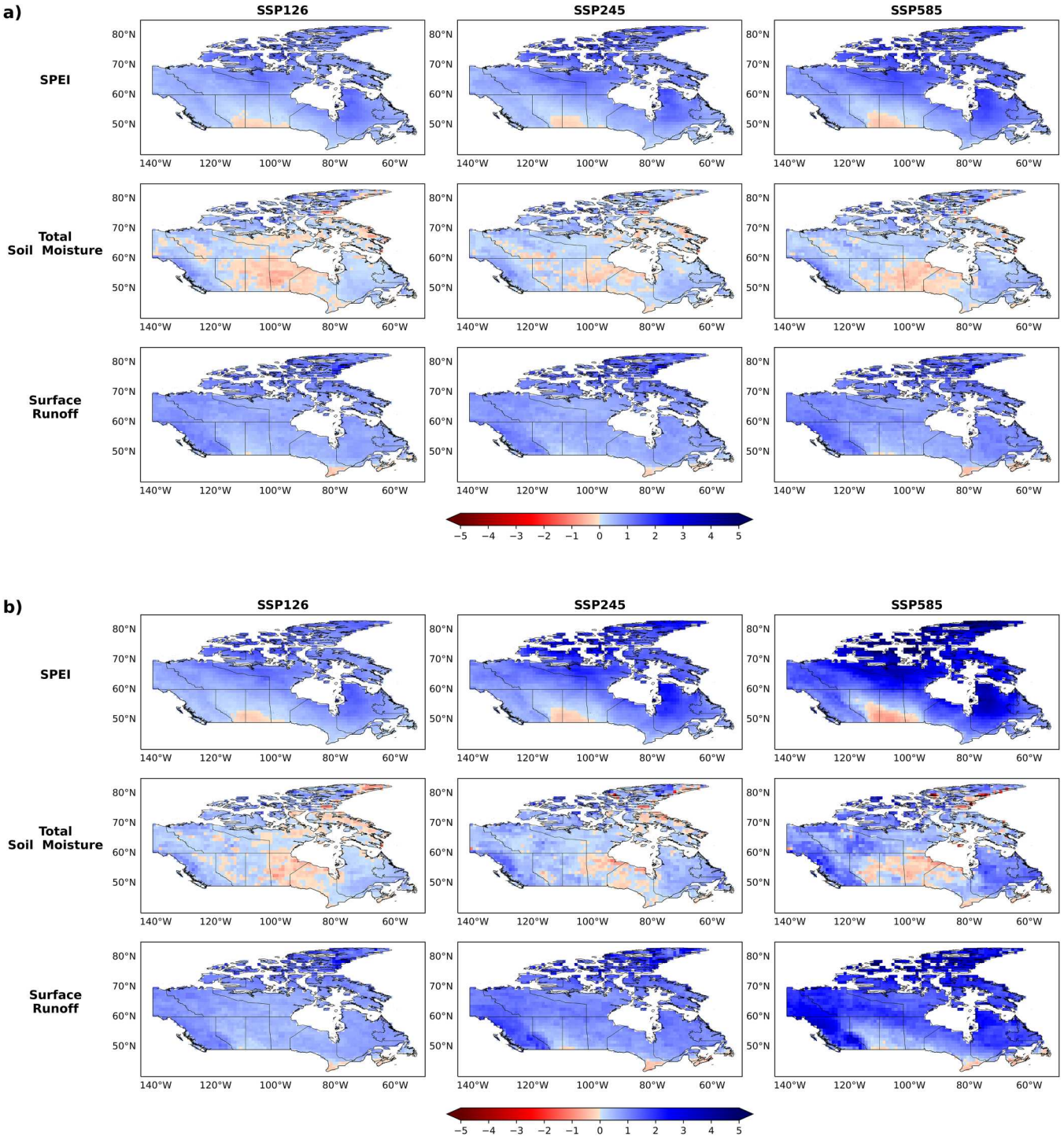


Fig. 6 Same as Fig. 2 except for cold season (October to March).

meteorological drought studies conducted on CMIP5 and CMIP6 results (e.g. Bonsal et al., 2020; Stewart et al., 2019; Tam, Bonsal et al., 2023). This pattern covers a greater portion of the country during the warm season (Figs 4 and 5) and is most widespread and severe during summer (Fig. 9). In spring, the driest conditions are more northward (Fig. 8). For all of these aforementioned periods, areas that are currently dry (i.e. have a moisture deficit as represented by $P$ minus PET; Fig. 1) are projected to become even drier thus exacerbating drought conditions. During the cold season (Figs 6 and 7), drier conditions are projected to slightly increase only over the extreme southern Prairies. In autumn, this region expands to cover most of the three Prairie provinces (Fig. 10). The Canadian Prairies are already prone to

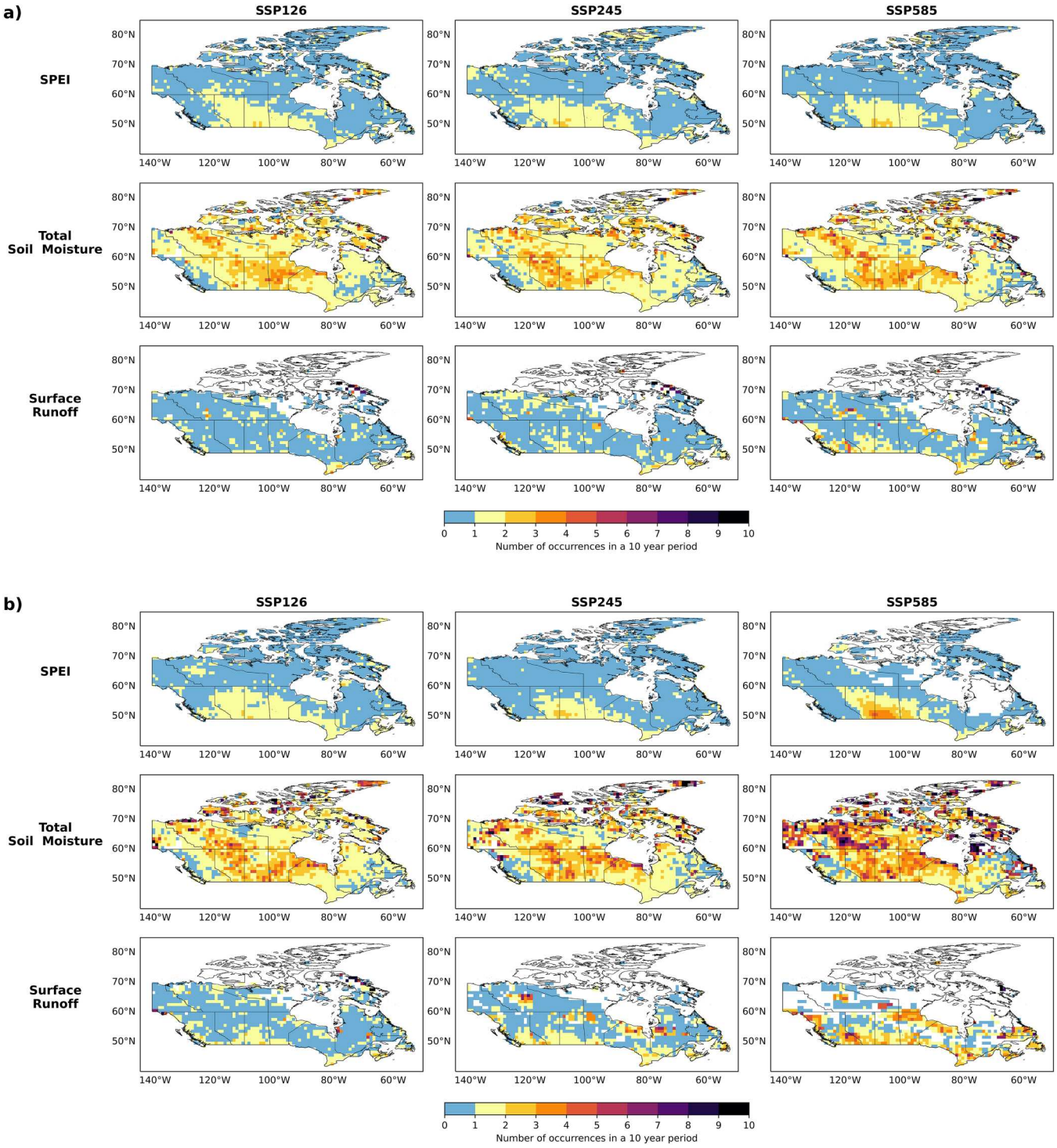


Fig. 7 Same as Fig. 3 except for cold season (October to March).

droughts and these results corroborate many past studies that suggest conditions will worsen under a warmer climate with an increase in the frequency and intensity of meteorological droughts, including multi-year and extreme droughts (Bonsal et al., 2013; 2020; Masud et al., 2017; PaiMazumder et al., 2013; Tam, Bonsal et al., 2023).

Total soil moisture, as represented by SSI, is projected to decrease over similar regions when compared to SPEI, but with smaller intensity. Annually, Fig. 2 shows reduced total soil moisture amounts covering parts of central Canada while Fig. 3 suggests more extreme droughts in the Prairies and the Northwest Territories. Warm season

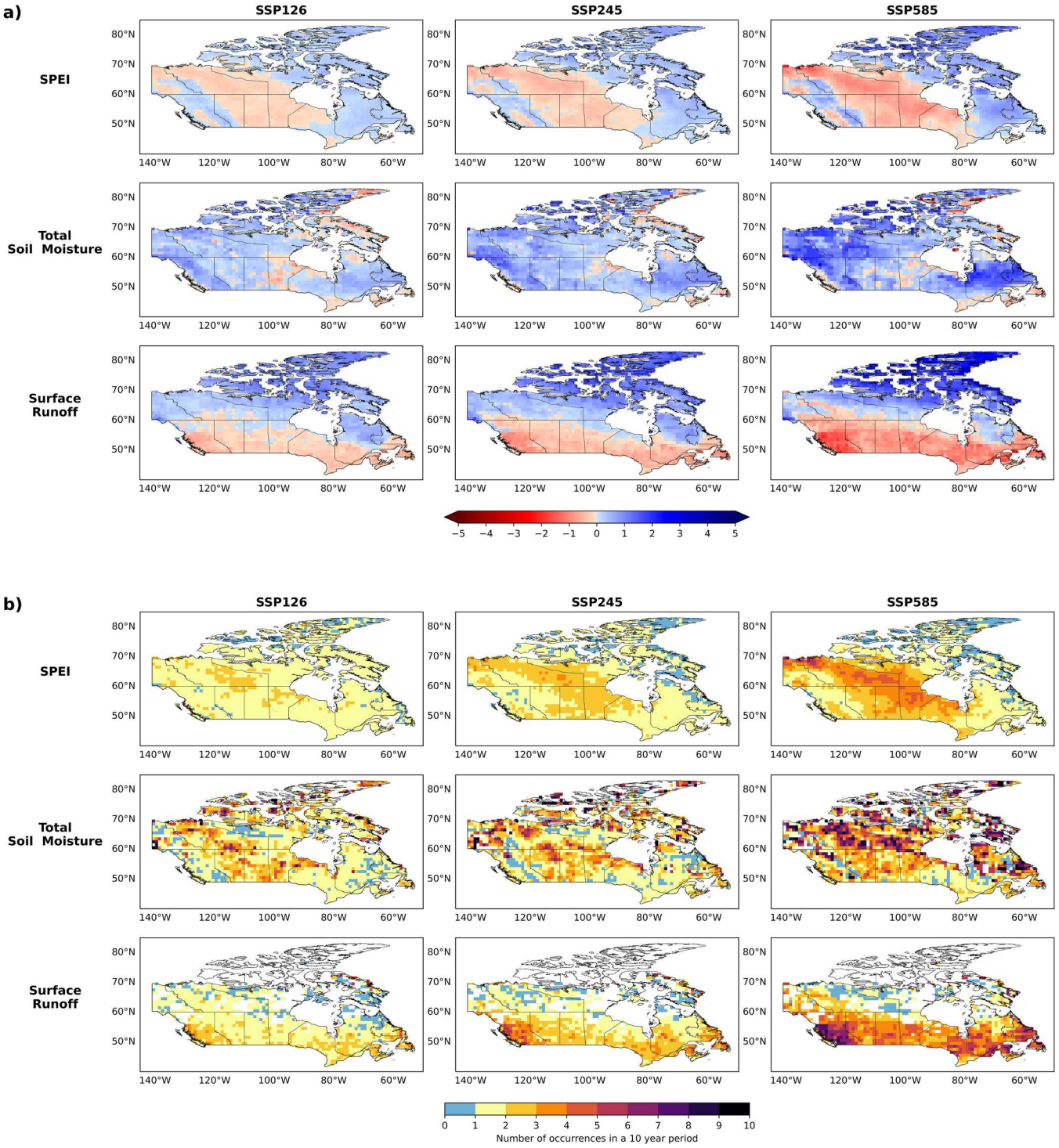


Fig. 8 Ensemble median (for all GCMs) projections of spring (March-April-May) SPEI, SSI, and SRI using SSPs 1-2.6, 2-4.5, and 5-8.5 for the period 2081–2100: (a) average changes and (b) changes to baseline (1950–2014) 1 in 10-year drought occurrences.

changes are similar, but drying is slightly more amplified and covers a larger portion of the country (Figs 4 and 5). These results are consistent with the spatial patterns of increased warm season total soil moisture drying under higher emission scenarios in Cook et al. (2020). During summer, changes are again more amplified when compared to annual and warm season projections (Fig 9). Autumn SSI also show projected drying over large regions of Canada (Fig 10), but the intensity and spatial extent are lower than summer. The cold season and spring show the least amount of change in agricultural drought (Figs 6–8). Climatologically, Fig. 1 shows that annual total soil moisture

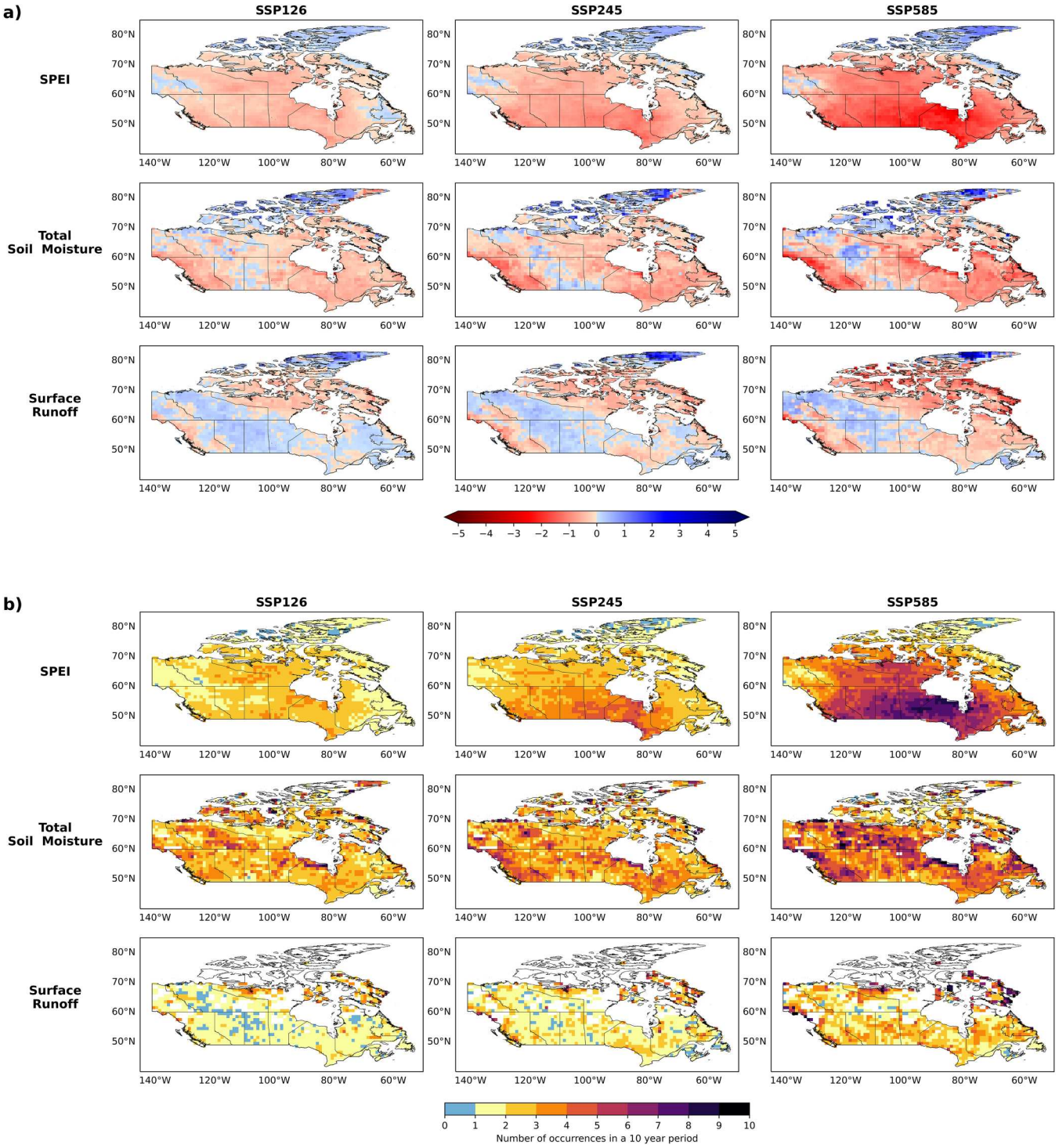


Fig. 9 Same as Fig. 8 except for summer (June-July-August).

is more varied with higher averages in central British Columbia, western Northwest Territories, northern Alberta, and along the southern coast of Hudson Bay, and rather uniform across the country for seasonal and 6-month periods. Lower values are consistently observed in southern Alberta and Saskatchewan and southern Ontario. On an annual basis, lower SSI and increases in 1 in 10-year droughts are projected for some regions of the country, with hotspots in 1 in 10-year droughts over parts of the Prairies and much of the Northwest Territories (Figs 2 and 3). Some of these hotspots differ from those associated with SPEI, which tend to be concentrated across the southern

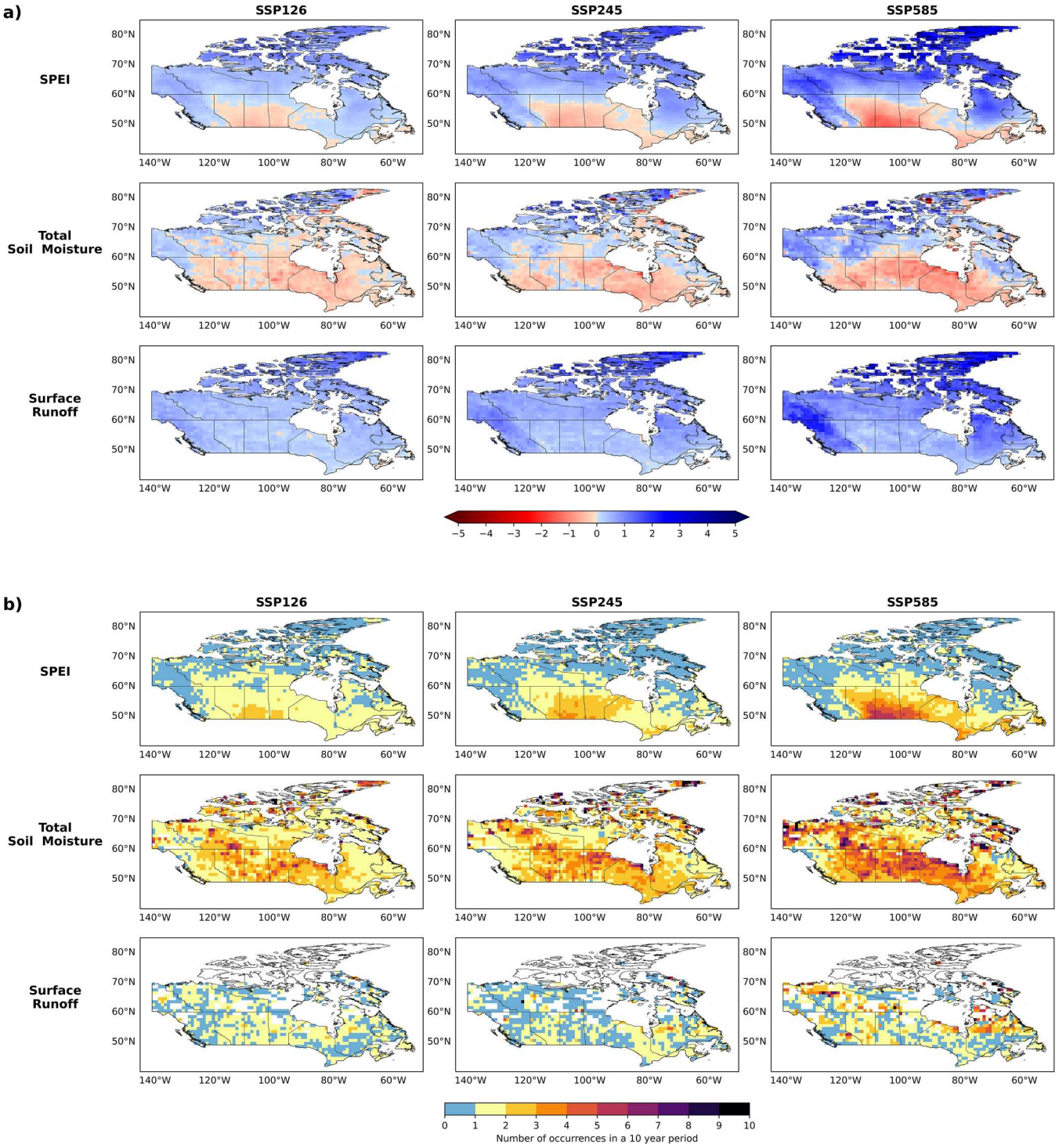


Fig. 10 Same as Fig. 8 except for autumn (September-October-November).

Prairies. Reasons for these differences in projected hotspot regions are not clear but are likely related to these changes being relative to the baseline conditions in Fig. 1 (which generally show higher amounts of soil moisture in most of these hotspot regions compared to areas such as the southern Prairies). As a result, the smaller relative changes across the southern Prairies still signify considerable drying in these current moisture-limited regions. This is corroborated by regional studies over the Prairies that found that increased warming will lead to an increase in drought frequency and greater soil moisture deficits (Chipanshi et al., 2022; Zare et al., 2023).

Hydrological conditions, as represented by SRI, show the least change among all the indicators. On a 12-month basis, this study showed that slightly drier conditions are evident throughout the approximate southern third of the country, while the rest of Canada is associated with wetter conditions that amplify in a northern direction (Figs 2 and 3). There is more pronounced projected drying during the warm season, especially in British Columbia, Ontario, and most of Quebec (Figs 4 and 5); similar to the spatial patterns of projected surface runoff drying in Cook et al. (2020). This pattern is also evident in spring (Fig. 8) but less so in summer (Fig. 9), which shows a variable pattern across the country. Both the cold season (Figs 6 and 7) and autumn (Fig. 10) show no future surface runoff decreases across almost the entire country; rather, surpluses in surface runoff are projected with spatial patterns similar to Cook et al. (2020).

Climatologically, Fig. 1 reveals that annual surface runoff is highest on the west and east coasts and lowest on the Prairies. Seasonally, spring has the highest amounts, which is reflective of the spring freshet and snowmelt. The fact that much of southern Canada, and in particular British Columbia, Ontario, and most of Quebec show the greatest changes in spring (Fig. 8) suggests that the critical runoff during this period is going to be lower and likely less reliable. This is consistent with the projected increases in snow drought and subsequent runoff projections by Shrestha et al. (2021). Similarly, a regional study over British Columbia found that increased snow droughts under increased anthropogenic warming can result in summer streamflow drought conditions (Dierauer et al., 2021). Projected runoff changes are still amplified for higher SSPs and during the late century, but less so than those associated with SPEI and to a lesser degree, total soil moisture. Likewise, Vicente-Serrano et al. (2020) found that SRI projected a lower increase (by ∼20%) in global land drying compared to meteorological and agricultural drought indices. In contrast, another global study found greater drying projected among hydrological and agricultural indices than meteorological, though that latter did not incorporate projected changes in evapotranspiration (Cook et al., 2020); highlighting the importance of PET in future meteorological drought projections (Vicente-Serrano, Beguería, & López-Moreno, 2010; Jeong et al., 2014).

The large-scale nature of this study along with the uncertainty associated with climate models introduce some limitations to this assessment. For example, GCMs vary in their representation of earth processes and as a result, will have biases in their output. While the study assessed multiple drought indices using an ensemble of multi-model output, quantifying uncertainty to some extent, there is still internal variability and scenario uncertainty embedded in the findings. Furthermore, there are model uncertainties on how drought processes may respond to a changing climate and how they are influenced by naturally occurring decadal-scale variability. One approach to reduce some uncertainty is to average results spatially and temporally from multiple models. While this may provide more robust results across a larger scale, local scale variability in variables such as soil moisture and runoff may be masked out. Higher resolution projections may provide more detail in future changes, though uncertainty increases as projections go from global scale to regional to local scale (Hawkins & Sutton, 2009). Another point to consider is that some climate model variables are more robust than others. CMIP6 temperature projections, for example, are generally very consistent across the models (Lee et al., 2021). Plots of CMIP6 soil moisture projections in the IPCC Sixth Assessment Report show lower model agreement across most of Canada, while there is high model agreement for runoff projections across most of Canada (Arias et al., 2021). Such aspects should be kept in consideration when interpreting the results of the present study. Also, the present study looked at seasonal, semi-annual, and annual future drought events. Other durations of droughts, such as 'flash droughts' or multi-year droughts, are also important to consider but were beyond the scope of the study. Lastly, while the present study shows novel results that could inform nation-wide adaptation strategies, further assessments and more localized scales are required.

## 5 Conclusions

The preceding attempted to answer the question, "Do meteorological, agricultural, and hydrological indicators all point to an increased frequency and intensity of droughts across Canada under a changing climate?".

Results revealed that the answer to this question depends on the region and period under consideration. Annually, all three drought indicators are projected to decrease across most of the country, particularly at the end of century under higher emissions. SPEI and total soil moisture decreases tend to be the greatest across the Prairies. Surface runoff shows the least change among all indicators (Figs 2 and 3). Projected drying covers a greater portion of the country during the warm season (April to September) when all three indicators show decreases across much of Canada (Figs 4 and 5). During summer, these widespread changes are only projected for SPEI and soil moisture (Fig. 9). In spring, hydrological drying encompasses most of the country south of 60 degrees, while SPEI decreases are amplified in the Prairies, Ontario and much of the Northwest Territories. The agricultural indicator shows the least amount of change (Fig. 8). For autumn, drying is only projected for meteorological and agricultural indicators with the former mainly being confined to the Prairies and the latter, covering much of the country south of 60° (Fig. 10). During the cold season, there is essentially no drying in any of the indicators (Figs 6 and 7).

In conclusion, analyses of meteorological, agricultural, and hydrological drought indicators shed greater insight into the range of regionally heterogeneous responses to human-induced warming in Canada. Standardization also allowed for direct comparison among the three indices, revealing some key similarities and differences among the various

drought types across the nation. While these results are consistent with other meteorological drought studies in Canada (e.g. Bonsal et al., 2020; Dibike et al., 2017; Tam, Bonsal et al. 2023), the present study provides novel insight on future nation-wide hydrological and agricultural drought conditions, which, to our knowledge, is currently limited in present literature. Such knowledge will help inform anticipated impacts and nation-wide adaptation measures for Canadians under a range of future climate scenarios. CMIP6 datasets described here are available for download through Environment and Climate Change Canada's Canadian Climate Data and Scenarios (CCDS) site (Environment and Climate Change Canada, 2024).

## Acknowledgements

We thank the reviewers for their constructive comments and suggestions that helped improve the manuscript. We acknowledge the international modelling centres, the Program for Climate Model Diagnosis and Intercomparison, the World Climate Research Program, and the Coupled Model Intercomparison Project for their roles in making available GCM datasets.

## Disclosure statement

No potential conflict of interest was reported by the author(s).

## References

Arias, P., Bellouin, N., Coppola, E., Jones, R., Krinner, G., Marotzke, J., Naik, V., Palmer, M., Plattner, G.-K., & Rogelj, J. (2021). *Climate change 2021: The physical science basis*. Contribution of Working Group I to the Sixth Assessment Report of the Intergovernmental Panel on Climate Change; Technical Summary.

Arora, V. K., & Boer, G. J. (2001). Effects of simulated climate change on the hydrology of major river basins. *Journal of Geophysical Research: Atmospheres*, *106*(D4), 3335–3348. https://doi.org/10.1029/2000JD900620

Arora, V. K., Lima, A., & Shrestha, R. (2025). The effect of climate change on the simulated streamflow of six Canadian rivers based on the CanRCM4 regional climate model. *Hydrology and Earth System Sciences, 29*(1), 291–312. https://doi.org/10.5194/hess-29-291-2025.

Beguería, S., Vicente-Serrano, S. M., Reig, F., & Latorre, B. (2014). Standardized precipitation evapotranspiration index (SPEI) revisited: Parameter fitting, evapotranspiration models, tools, datasets and drought monitoring. *International Journal of Climatology*, *34*(10), 3001–3023. https://doi.org/10.1002/joc.3887

Berg, A., Sheffield, J., & Milly, P. C. (2017). Divergent surface and total soil moisture projections under global warming. *Geophysical Research Letters*, *44*(1), 236–244. https://doi.org/10.1002/2016GL071921

Bi, D., Dix, M., Marsland, S., O'farrell, S., Sullivan, A., Bodman, R., Law, R., Harman, I., Srbinovsky, J., & Rashid, H. A. (2020). Configuration and spin-up of ACCESS-CM2, the new generation Australian community climate and earth system simulator coupled model. *Journal of Southern Hemisphere Earth Systems Science*, *70*(1), 225–251. https://doi.org/10.1071/ES19040

Bonsal, B. R., Aider, R., Gachon, P., & Lapp, S. (2013). An assessment of Canadian prairie drought: Past, present, and future. *Climate Dynamics*, *41*(2), 501–516. https://doi.org/10.1007/s00382-012-1422-0

Bonsal, B. R., Liu, Z., Wheaton, E., & Stewart, R. (2020). Historical and projected changes to the stages and other characteristics of severe Canadian Prairie droughts. *Water*, *12*(12), 3370. https://doi.org/10.3390/w12123370

Bonsal, B. R., Peters, D. L., Seglenieks, F., Rivera, A., & Berg, A. (2019). Changes in freshwater availability across Canada; Chapter 6 in *Canada's Changing Climate Report*, (ed.) E. Bush and D.S. Lemmen; Government of Canada, Ottawa, Ontario, 261–342.

Bonsal, B. R., Wheaton, E. E., Chipanshi, A. C., Lin, C., Sauchyn, D. J., & Wen, L. (2011). Drought research in Canada: A review. *Atmosphere-Ocean*, *49*(4), 303–319. https://doi.org/10.1080/07055900.2011.555103

Boucher, O., Servonnat, J., Albright, A. L., Aumont, O., Balkanski, Y., Bastrikov, V., Bekki, S., Bonnet, R., Bony, S., & Bopp, L. (2020). Presentation and evaluation of the IPSL-CM6A-LR climate model. *Journal of Advances in Modeling Earth Systems*, *12*(7), e2019MS002010. https://doi.org/10.1029/2019MS002010

Budhathoki, S., Rokaya, P., & Lindenschmidt, K.-E. (2022). Impacts of future climate on the hydrology of a transboundary river basin in northeastern North America. *Journal of Hydrology*, *605*, 127317. https://doi.org/10.1016/j.jhydrol.2021.127317

Chen, X., Zhao, P., Ouyang, L., Zhu, L., Ni, G., & Schäfer, K. V. (2020). Whole-plant water hydraulic integrity to predict drought-induced *Eucalyptus urophylla* mortality under drought stress. *Forest Ecology and Management*, *468*, 118179. https://doi.org/10.1016/j.foreco.2020.118179

Cherchi, A., Fogli, P. G., Lovato, T., Peano, D., Iovino, D., Gualdi, S., Masina, S., Scoccimarro, E., Materia, S., & Bellucci, A. (2019). Global mean climate and main patterns of variability in the CMCC-CM2 coupled model. *Journal of Advances in Modeling Earth Systems*, *11*(1), 185–209. https://doi.org/10.1029/2018MS001369

Chipanshi, A., Berry, M., Zhang, Y., Qian, B., & Steier, G. (2022). Agroclimatic indices across the Canadian Prairies under a changing climate and their implications for agriculture. *International Journal of Climatology*, *42*(4), 2351–2367. https://doi.org/10.1002/joc.7369

Cook, B. I., Mankin, J. S., Marvel, K., Williams, A. P., Smerdon, J. E., & Anchukaitis, K. J. (2020). Twenty-first century drought projections in the CMIP6 forcing scenarios. *Earth's Future*, *8*(6), e2019EF001461. https://doi.org/10.1029/2019EF001461

Derksen, C., Burgess, D., Duguay, C., Howell, S., Mudryk, L., Smith, S., Thackeray, C., & Kirchmeier-Young, M. (2019). Changes in snow, ice, and permafrost across Canada; Chapter 5 in *Canada's Changing Climate Report*, (ed.) E. Bush and D.S. Lemmen; Government of Canada, Ottawa, Ontario, 194–260.

Dibike, Y., Prowse, T., Bonsal, B., & O'Neil, H. (2017). Implications of future climate on water availability in the western Canadian river basins. *International Journal of Climatology*, *37*(7), 3247–3263. https://doi.org/10.1002/joc.4912

Dierauer, J. R., Allen, D. M., & Whitfield, P. H. (2021). Climate change impacts on snow and streamflow drought regimes in four ecoregions of British Columbia. *Canadian Water Resources Journal / Revue Canadienne Des Ressources Hydriques*, *46*(4), 168–193. https://doi.org/10.1080/07011784.2021.1960894

Döscher, R., Acosta, M., Alessandri, A., Anthoni, P., Arsouze, T., Bergman, T., Bernardello, R., Boussetta, S., Caron, L.-P., & Carver, G. (2022). The EC-Earth3 earth system model for the coupled model intercomparison project 6. *Geoscientific Model Development*, *15*(7), 2973–3020. https://doi.org/10.5194/gmd-15-2973-2022

Dunne, J. P., Horowitz, L. W., Adcroft, A. J., Ginoux, P., Held, I. M., John, J. G., Krasting, J. P., Malyshev, S., Naik, V., & Paulot, F. (2020). The GFDL earth system model version 4.1 (GFDL-ESM 4.1): Overall coupled model description and simulation characteristics. *Journal of Advances in Modeling Earth Systems*, *12*(11), e2019MS002015. https://doi.org/10.1029/2019MS002015

Environment and Climate Change Canada. (2024). *Canadian climate data and scenarios*. https://climate-scenarios.canada.ca

Eyring, V., Bony, S., Meehl, G. A., Senior, C. A., Stevens, B., Stouffer, R. J., & Taylor, K. E. (2016). Overview of the coupled model intercomparison project phase 6 (CMIP6) experimental design and organization. *Geoscientific Model Development*, *9*(5), 1937–1958. https://doi.org/10.5194/gmd-9-1937-2016

Guttman, N. B. (1994). On the sensitivity of sample L moments to sample size. *Journal of Climate*, *7*(6), 1026–1029. https://doi.org/10.1175/1520-0442(1994)007<1026:OTSOSL>2.0.CO;2

Guttman, N. B. (1999). Accepting the standardized precipitation index: A calculation algorithm. *JAWRA Journal of the American Water Resources Association*, *35*(2), 311–322. https://doi.org/10.1111/j.1752-1688.1999.tb03592.x

Hajima, T., Watanabe, M., Yamamoto, A., Tatebe, H., Noguchi, M. A., Abe, M., Ohgaito, R., Ito, A., Yamazaki, D., & Okajima, H. (2020). Development of the MIROC-ES2L Earth system model and the evaluation of biogeochemical processes and feedbacks. *Geoscientific Model Development*, *13*(5), 2197–2244. https://doi.org/10.5194/gmd-13-2197-2020

Hawkins, E., & Sutton, R. (2009). The potential to narrow uncertainty in regional climate predictions. *Bulletin of the American Meteorological Society*, *90*(8), 1095–1108. https://doi.org/10.1175/2009BAMS2607.1

Hayat, F., Ahmed, M. A., Zarebanadkouki, M., Cai, G., & Carminati, A. (2019). Measurements and simulation of leaf xylem water potential and root water uptake in heterogeneous soil water contents. *Advances in Water Resources*, *124*, 96–105. https://doi.org/10.1016/j.advwatres.2018.12.009

Islam, S. U., Curry, C. L., Déry, S. J., & Zwiers, F. W. (2019). Quantifying projected changes in runoff variability and flow regimes of the Fraser River Basin, British Columbia. *Hydrology and Earth System Sciences*, *23*(2), 811–828. https://doi.org/10.5194/hess-23-811-2019

Jehanzaib, M., Shah, S. A., Yoo, J., & Kim, T.-W. (2020). Investigating the impacts of climate change and human activities on hydrological drought using non-stationary approaches. *Journal of Hydrology*, *588*, 125052. https://doi.org/10.1016/j.jhydrol.2020.125052

Jeong, D. I., Sushama, L., & Naveed Khaliq, M. (2014). The role of temperature in drought projections over North America. *Climatic Change*, *127*(2), 289–303. https://doi.org/10.1007/s10584-014-1248-3

Kuhlbrodt, T., Jones, C. G., Sellar, A., Storkey, D., Blockley, E., Stringer, M., Hill, R., Graham, T., Ridley, J., & Blaker, A. (2018). The low-resolution version of HadGEM3 GC3.1: Development and evaluation for global climate. *Journal of Advances in Modeling Earth Systems*, *10*(11), 2865–2888. https://doi.org/10.1029/2018MS001370

Kumar, S., Newman, M., Wang, Y., & Livneh, B. (2019). Potential reemergence of seasonal soil moisture anomalies in North America. *Journal of Climate*, *32*(10), 2707–2734. https://doi.org/10.1175/JCLI-D-18-0540.1

Lee, J.-Y., Marotzke, J., Bala, G., Cao, L., Corti, S., Dunne, J. P., Engelbrecht, F., Fischer, E., Fyfe, J. C., & Jones, C. (2021). *Future global climate: Scenario-based projections and near-term information*. IPCC.

Lee, W.-L., Wang, Y.-C., Shiu, C.-J., Tsai, I., Tu, C.-Y., Lan, Y.-Y., Chen, J.-P., Pan, H.-L., & Hsu, H.-H. (2020). Taiwan Earth system model version 1: Description and evaluation of mean state. *Geoscientific Model Development*, *13*(9), 3887–3904. https://doi.org/10.5194/gmd-13-3887-2020

Lovato, T., Peano, D., Butenschön, M., Materia, S., Iovino, D., Scoccimarro, E., Fogli, P. G., Cherchi, A., Bellucci, A., & Gualdi, S. (2022). CMIP6 simulations with the CMCC Earth system model (CMCC-ESM2). *Journal of Advances in Modeling Earth Systems*, *14*(3), e2021MS002814. https://doi.org/10.1029/2021MS002814

Masud, M. B., Khaliq, M. N., & Wheater, H. S. (2017). Future changes to drought characteristics over the Canadian Prairie provinces based on NARCCAP multi-RCM ensemble. *Climate Dynamics*, *48*(7), 2685–2705. https://doi.org/10.1007/s00382-016-3232-2

Mauritsen, T., Bader, J., Becker, T., Behrens, J., Bittner, M., Brokopf, R., Brovkin, V., Claussen, M., Crueger, T., & Esch, M. (2019). Developments in the MPI-M Earth system model version 1.2 (MPI-ESM1. 2) and its response to increasing $CO_2$. *Journal of Advances in Modeling Earth Systems*, *11*(4), 998–1038. https://doi.org/10.1029/2018MS001400

McKee, T. B., Doesken, N. J., & Kleist, J. (1993). The relationship of drought frequency and duration to time scales. *Proceedings of the 8th Conference on Applied Climatology*, *17*(22), 179–183.

Meinshausen, M., Nicholls, Z. R., Lewis, J., Gidden, M. J., Vogel, E., Freund, M., Beyerle, U., Gessner, C., Nauels, A., & Bauer, N. (2020). The shared socio-economic pathway (SSP) greenhouse gas concentrations and their extensions to 2500. *Geoscientific Model Development*, *13*(8), 3571–3605. https://doi.org/10.5194/gmd-13-3571-2020

Mizuta, R., Yoshimura, H., Murakami, H., Matsueda, M., Endo, H., Ose, T., Kamiguchi, K., Hosaka, M., Sugi, M., & Yukimoto, S. (2012). Climate simulations using MRI-AGCM3.2 with 20-km grid. *Journal of the Meteorological Society of Japan Ser. II*, *90A*, 233–258.

Müller, W. A., Jungclaus, J. H., Mauritsen, T., Baehr, J., Bittner, M., Budich, R., Bunzel, F., Esch, M., Ghosh, R., & Haak, H. (2018). A higher-resolution version of the Max Planck Institute earth system model (MPI-ESM1.2-HR). *Journal of Advances in Modeling Earth Systems*, *10*(7), 1383–1413. https://doi.org/10.1029/2017MS001217

PaiMazumder, D., Sushama, L., Laprise, R., Khaliq, M. N., & Sauchyn, D. (2013). Canadian RCM projected changes to short- and long-term drought characteristics over the Canadian Prairies. *International Journal of Climatology*, *33*(6), 1409–1423. https://doi.org/10.1002/joc.3521

Saint-Martin, D., Geoffroy, O., Voldoire, A., Cattiaux, J., Brient, F., Chauvin, F., Chevallier, M., Colin, J., Decharme, B., & Delire, C. (2021). Tracking changes in climate sensitivity in CNRM climate models. *Journal of Advances in Modeling Earth Systems*, *13*(6), e2020MS002190. https://doi.org/10.1029/2020MS002190

Schnorbus, M. A. (2020). *VIC glacier (VIC-GL) – Model set-up and deployment for the peace, Fraser, and Columbia, VIC generation 2 deployment report* (Vol. 6, p. 73). Pacific Climate Impacts Consortium, University of Victoria. https://www.pacificclimate.org/sites/default/files/publications/VIC-Gen2-DR-V6_Schnorbus_2020_model_deployment.pdf

Seiler, C., Melton, J. R., Arora, V. K., & Wang, L. (2021). CLASSIC v1.0: The open-source community successor to the Canadian land surface scheme (CLASS) and the Canadian terrestrial ecosystem model (CTEM) – Part 2: Global benchmarking. *Geoscientific Model Development*, *14*(5), 2371–2417. https://doi.org/10.5194/gmd-14-2371-2021

Seland, Ø, Bentsen, M., Oliviè, D. J. L., Toniazzo, T., Gjermundsen, A., Graff, L. S., Debernard, J. B., Gupta, A. K., He, Y.-C., & Kirkevåg, A. (2020). *Overview of the Norwegian earth system model (NorESM2) and key climate response of CMIP6 DECK, historical, and scenario simulations*.

Sellar, A. A., Jones, C. G., Mulcahy, J. P., Tang, Y., Yool, A., Wiltshire, A., O'connor, F. M., Stringer, M., Hill, R., & Palmieri, J. (2019). UKESM1: Description and evaluation of the U.K. Earth system model. *Journal of Advances in Modeling Earth Systems*, *11*(12), 4513–4558. https://doi.org/10.1029/2019MS001739

Séférian, R., Nabat, P., Michou, M., Saint-Martin, D., Voldoire, A., Colin, J., Decharme, B., Delire, C., Berthet, S., & Chevallier, M. (2019). Evaluation of CNRM Earth system model, CNRM-ESM2-1: Role of Earth system processes in present-day and future climate. *Journal of Advances in Modeling Earth Systems*, *11*(12), 4182–4227. https://doi.org/10.1029/2019MS001791

Shrestha, R. R., Bonsal, B. R., Bonnyman, J. M., Cannon, A. J., & Najafi, M. R. (2021). Heterogeneous snowpack response and snow drought occurrence across river basins of northwestern North America under 1.0°C to 4.0°C global warming. *Climatic Change*, *164*(3-4), 1–21. https://doi.org/10.1007/s10584-021-02968-7

Shrestha, R. R., Cannon, A. J., Schnorbus, M. A., & Alford, H. (2019). Climatic controls on future hydrologic changes in a subarctic river basin in Canada. *Journal of Hydrometeorology*, *20*(9), 1757–1778. https://doi.org/10.1175/JHM-D-18-0262.1

Sigmond, M., Anstey, J., Arora, V., Digby, R., Gillett, N., Kharin, V., Merryfield, W., Reader, C., Scinocca, J., Swart, N., Virgin, J., Abraham, C., Cole, J., Lambert, N., Lee, W.-S., Liang, Y., Malinina, E., Rieger, L., von Salzen, K., … Yang, D. (2023). Improvements in the Canadian

Earth system model (CanESM) through systematic model analysis: CanESM5.0 and CanESM5.1. *Geoscientific Model Development*, *16*(22), 6553–6591. https://doi.org/10.5194/gmd-16-6553-2023

Stadnyk, T. A., Tefs, A., Broesky, M., Déry, S. J., Myers, P. G., Ridenour, N. A., Koenig, K., Vonderbank, L., & Gustafsson, D. (2021). Changing freshwater contributions to the Arctic: A 90-year trend analysis (1981–2070). *Elementa: Science of the Anthropocene*, *9*(1), 00098. https://doi.org/10.1525/elementa.2020.00098

Stewart, R. E., Szeto, K. K., Bonsal, B. R., Hanesiak, J. M., Kochtubajda, B., Li, Y., Thériault, J. M., DeBeer, C. M., Tam, B. Y., & Li, Z. (2019). Summary and synthesis of changing cold regions network (CCRN) research in the interior of western Canada – Part 1: Projected climate and meteorology. *Hydrology and Earth System Sciences*, *23*(8), 3437–3455. https://doi.org/10.5194/hess-23-3437-2019

Swart, N. C., Cole, J. N., Kharin, V. V., Lazare, M., Scinocca, J. F., Gillett, N. P., Anstey, J., Arora, V., Christian, J. R., & Hanna, S. (2019). The Canadian Earth system model version 5 (CanESM5.0.3). *Geoscientific Model Development*, *12*(11), 4823–4873. https://doi.org/10.5194/gmd-12-4823-2019

Tam, B., Bonsal, B., Zhang, X., Zhang, Q., & Rong, R. (2023). Assessing potential evapotranspiration methods in future drought projections across Canada. *Atmosphere-Ocean*, *62*(3), 1–13.

Tam, B. Y., Szeto, K., Bonsal, B., Flato, G., Cannon, A. J., & Rong, R. (2019). CMIP5 drought projections in Canada based on the standardized precipitation evapotranspiration index. *Canadian Water Resources Journal/Revue canadienne des ressources hydriques*, *44*(1), 90–107. https://doi.org/10.1080/07011784.2018.1537812

Tatebe, H., Ogura, T., Nitta, T., Komuro, Y., Ogochi, K., Takemura, T., Sudo, K., Sekiguchi, M., Abe, M., & Saito, F. (2019). Description and basic evaluation of simulated mean state, internal variability, and climate sensitivity in MIROC6. *Geoscientific Model Development*, *12*(7), 2727–2765. https://doi.org/10.5194/gmd-12-2727-2019

Tijdeman, E., Hannaford, J., & Stahl, K. (2018). Human influences on streamflow drought characteristics in England and Wales. *Hydrology and Earth System Sciences*, *22*(2), 1051–1064. https://doi.org/10.5194/hess-22-1051-2018

Van Loon, A. F. (2015). Hydrological drought explained. *WIREs Water*, *2*(4), 359–392. https://doi.org/10.1002/wat2.1085

Van Loon, A. F., Stahl, K., Di Baldassarre, G., Clark, J., Rangecroft, S., Wanders, N., Gleeson, T., Van Dijk, A. I., Tallaksen, L. M., & Hannaford, J. (2016). Drought in a human-modified world: Reframing drought definitions, understanding, and analysis approaches. *Hydrology and Earth System Sciences*, *20*(9), 3631–3650. https://doi.org/10.5194/hess-20-3631-2016

Vicente-Serrano, S. M., Beguería, S., & López-Moreno, J. I. (2010). A multiscalar drought index sensitive to global warming: The standardized precipitation evapotranspiration index. *Journal of Climate*, *23*(7), 1696–1718. https://doi.org/10.1175/2009JCLI2909.1

Vicente-Serrano, S. M., Domínguez-Castro, F., McVicar, T. R., Tomas-Burguera, M., Peña-Gallardo, M., Noguera, I., López-Moreno, J. I., Pena, D., & El Kenawy, A. (2020). Global characterization of hydrological and meteorological droughts under future climate change: The importance of timescales, vegetation-$CO_2$ feedbacks and changes to distribution functions. *International Journal of Climatology*, *40*(5), 2557–2567. https://doi.org/10.1002/joc.6350

Voldoire, A., Saint-Martin, D., Sénési, S., Decharme, B., Alias, A., Chevallier, M., Colin, J., Guérémy, J.-F., Michou, M., & Moine, M.-P. (2019). Evaluation of CMIP6 deck experiments with CNRM-CM6-1. *Journal of Advances in Modeling Earth Systems*, *11*(7), 2177–2213. https://doi.org/10.1029/2019MS001683

Volodin, E. M., Mortikov, E. V., Kostrykin, S. V., Galin, V. Y., Lykossov, V. N., Gritsun, A. S., Diansky, N. A., Gusev, A. V., & Iakovlev, N. G. (2017). Simulation of the present-day climate with the climate model INMCM5. *Climate Dynamics*, *49*(11-12), 3715–3734. https://doi.org/10.1007/s00382-017-3539-7

Volodin, E. M., Mortikov, E. V., Kostrykin, S. V., Galin, V. Y., Lykossov, V. N., Gritsun, A. S., Diansky, N. A., Gusev, A. V., Iakovlev, N. G., & Shestakova, A. A. (2018). Simulation of the modern climate using the INM-CM48 climate model. *Russian Journal of Numerical Analysis and Mathematical Modelling*, *33*(6), 367–374. https://doi.org/10.1515/rnam-2018-0032

Williams, K. D., Copsey, D., Blockley, E. W., Bodas-Salcedo, A., Calvert, D., Comer, R., Davis, P., Graham, T., Hewitt, H. T., & Hill, R. (2018). The Met office global coupled model 3.0 and 3.1 (GC3.0 and GC3.1) configurations. *Journal of Advances in Modeling Earth Systems*, *10*(2), 357–380. https://doi.org/10.1002/2017MS001115

Yukimoto, S., Kawai, H., Koshiro, T., Oshima, N., Yoshida, K., Urakawa, S., Tsujino, H., Deushi, M., Tanaka, T., & Hosaka, M. (2019). The meteorological research institute earth system model version 2.0, MRI-ESM2.0: Description and basic evaluation of the physical component. *Journal of the Meteorological Society of Japan. Ser. II*, *97*(5), 931–965. https://doi.org/10.2151/jmsj.2019-051

Zare, M., Azam, S., Sauchyn, D., & Basu, S. (2023). Assessment of meteorological and agricultural drought indices under climate change scenarios in the South Saskatchewan River Basin, Canada. *Sustainability*, *15*(7), 5907. https://doi.org/10.3390/su15075907

Zeng, J., Li, J., Lu, X., Wei, Z., Shangguan, W., Zhang, S., Dai, Y., & Zhang, S. (2022). Assessment of global meteorological, hydrological and agricultural drought under future warming based on CMIP6. *Atmospheric and Oceanic Science Letters*, *15*(1), 100143. https://doi.org/10.1016/j.aosl.2021.100143

Zhang, X., Tang, Q., Zhang, X., & Lettenmaier, D. P. (2014). Runoff sensitivity to global mean temperature change in the CMIP5 models. *Geophysical Research Letters*, *41*(15), 5492–5498. https://doi.org/10.1002/2014GL060382

Ziehn, T., Chamberlain, M. A., Law, R. M., Lenton, A., Bodman, R. W., Dix, M., Stevens, L., Wang, Y.-P., & Srbinovsky, J. (2020). The Australian earth system model: ACCESS-ESM1.5. *Journal of Southern Hemisphere Earth Systems Science*, *70*(1), 193–214. https://doi.org/10.1071/ES19035